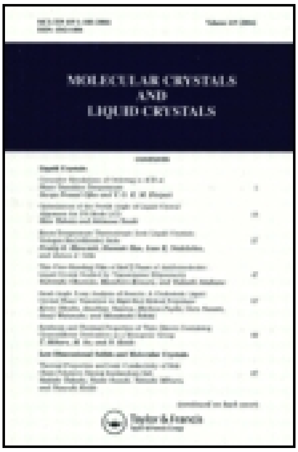

Molecular Crystals and Liquid Crystals
Publication details, including instructions for authors and subscription information:
http://www.tandfonline.com/loi/gmcl18

Director Patterns and Optical Performance of 2D-Inhomogeneously Deformed Nematic Liquid Crystal Layers

Mattias Schmidt [a]

[a] University Leipzig, Department of Physics, Linnestr. 5, 0-7010, Leipzig, Germany

Version of record first published: 24 Sep 2006.

To cite this article: Mattias Schmidt (1991): Director Patterns and Optical Performance of 2D-Inhomogeneously Deformed Nematic Liquid Crystal Layers, Molecular Crystals and Liquid Crystals, 206:1, 65-77

To link to this article: http://dx.doi.org/10.1080/00268949108037719

Mol. Cryst. Liq. Cryst., 1991, Vol. 206, pp. 65–77
Reprints available directly from the publisher
Photocopying permitted by license only

Printed in the United States of America

Director Patterns and Optical Performance of 2D-Inhomogeneously Deformed Nematic Liquid Crystal Layers

MATTIAS SCHMIDT
University Leipzig, Department of Physics, Linnestr. 5, 0-7010 Leipzig, Germany

(Received December 7, 1990; in final form February 2, 1991)

An original numerical computation of director configurations of a nematic liquid crystal layer in a two dimensional inhomogeneous (2D) electrical field is presented. In the calculation, a relaxation method is used to solve the corresponding differential equations and boundary value problems. The optical performance, as exemplified by the Fraunhofer diffraction, is then calculated.

The calculations involve the self-consistent coupling between the director deformation and the electrical field distribution and are applied to liquid crystal spatial light modulators. For the first time, the anisotropy of the modulation transfer function of a nematic liquid crystal light modulator is specified and its dependence on the device parameters as well as on the LC material constants is studied.

Keywords: liquid crystal displays, spatial light modulators, inhomogeneous electrical field, resolution capability, light diffraction, diffraction efficiency

INTRODUCTION

Usually, a nematic[1] liquid crystal display (LCD) is assumed to represent a stratified medium.[2] The corresponding one dimensional theory is well understood.[3] The calculation of the optical performance of a LCD splits into two steps. First, the distribution of the optical axis through the liquid crystal (LC) layer—called director pattern—is determined by means of the continuum theory. Many authors have investigated the director patterns in a one dimensional continuum approach, see, for example References 4–6. Second, the optical properties of the display are computed.

To solve Maxwells equations for the light propagation in stratified media, the 4×4 matrix formalism[2] is the most commonly used method.[3,7]

In many cases of practical interest the optical response of the LC depends on the distribution of a spatially non-uniform electric field that arises for instance from the pixel structure in matrix displays or from an intensity distribution on the photoconductor in liquid crystal spatial light modulators (SLMs).[8]

With the ever decreasing scale of structures of the pixels in matrix displays, a calculation is needed to investigate the limiting resolution capabilities of the liquid crystal layer and its optical performance, and to study the director patterns in the spatially inhomogeneous electrical field arising from the structure of the electrodes.

We present here an original numerical computation of director configurations of a nematic liquid crystal layer in a two dimensional, inhomogeneous (2D), electrical field. In the calculation a relaxation method is used to solve the corresponding differential equations and boundary value problems. The optical performance, as exemplified by the Fraunhofer diffraction, is then calculated.

The calculations involve the self-consistent coupling between the director deformation and the electrical field distribution and are applied to LC light modulators.[8] For the first time, the anisotropy of the modulation transfer function of a nematic LC light modulator is specified and its dependence on the device parameters as well as on the LC material constants is studied.

The results are compared with an analytical approach that was recently given by Chigrinov,[9] where the coupling between director variation and electric field distribution was neglected and only small deformations were considered.

CALCULATION OF DIRECTOR PATTERNS

We consider a nematic liquid crystal layer of thickness d located between the planes $z = 0$ and $z = d$ of a Cartesian coordinate system. The direction of the optical axis (director) is usually described by means of the tilt angle θ (measured from the layer plane) and the twist angle ϕ.[10] The dielectric constants parallel and perpendicular to the director are denoted by $\varepsilon_\parallel$ and $\varepsilon_\perp$. The elastic constants for splay, twist and bend are given by K_1, K_2 and K_3. The tilt angle at both surfaces is denoted by θ_o and we assume strong anchoring. In the calculations, we restrict ourselves to the two-dimensional case and assume that the electrical field and the director pattern are invariant in the y-direction. We further demand that the variation of the director is performed in a plane, that means that the twist angle ϕ is a constant. This assumption is exactly valid only if the director lies in the plane of the field inhomogeneity, i.e., if $\phi = 0$. In the other cases, the director could experience a "twisting torque" near the boundaries of the striped electrodes; this has been neglected for simplicity in the following treatment.

Our aim is the computation of the director distribution $\theta(x, z)$ and the electric potential $V(x, z)$ with the boundary value conditions:

$$\theta(x, z = 0) = \theta_o \qquad \theta(x, z = d) = \theta_o \tag{1}$$

$$V(x, z = 0) = V_o \qquad V(x, z = d) = V_1(x) \tag{2}$$

Here the function $V_1(x)$ is an arbitrary one dimensional periodic voltage distribution with a grating constant g. Hence, the director pattern will be periodic

$$\theta(x + g, z) = \theta(x, z) \qquad V(x + g, z) = V(x, z) \tag{3}$$

and we consider the unit cell with $0 \leq x \leq g$ and $0 \leq z \leq d$.

To study the possible equilibrium director configurations the free enthalpy

$$G = \int_0^g \int_0^d (w_{\text{elast}} - w_{\text{el}})\, dxdz \tag{4}$$

must be minimized under the conditions (1)–(3). Here w_{elast} and w_{el} denote the energy densities of the elastic deformation and the electric field, respectively. The variational principle leads to a set of two differential equations

$$\frac{\partial \bar{g}}{\partial \theta} - \frac{\partial}{\partial x}\frac{\partial \bar{g}}{\partial \theta_x} - \frac{\partial}{\partial z}\frac{\partial \bar{g}}{\partial \theta_z} = 0 \tag{5}$$

$$\frac{\partial}{\partial x}\frac{\partial \bar{g}}{\partial V_x} + \frac{\partial}{\partial z}\frac{\partial \bar{g}}{\partial V_z} = 0 \tag{6}$$

with the abbreviations $\bar{g} = w_{\text{elast}} - w_{\text{el}}$, $\theta_\alpha = \partial\theta/\partial\alpha$ and $V_\alpha = \partial V/\partial\alpha$ ($\alpha = x, z$).

In the following, we restrict ourselves to two principal cases of director alignment in the xz-plane of the field inhomogeneity ($\phi = 0$) or perpendicular to it ($\phi = 90°$).

First Case: $\phi = 0$

The densities of the elastic deformation and the electric field are given by

$$w_{\text{elast}} = \frac{1}{2}(K_1 s^2\theta + K_3 c^2\theta)\theta_x^2 + \frac{1}{2}(K_1 c^2\theta + K_3 s^2\theta)\theta_z^2 + (K_3 - K_1)s\theta c\theta\theta_x\theta_z \tag{7}$$

$$w_{\text{el}} = \frac{1}{2}\varepsilon_0(\varepsilon_\perp(V_x^2 + V_z^2) + \Delta\varepsilon(V_x^2 c^2\theta + 2V_xV_z s\theta c\theta + V_z^2 s^2\theta)) \tag{8}$$

Here the letters s and c denote the sin and cos function, respectively. Substitution of (7), (8) into the Eulerian equations gives

$$\begin{aligned}\theta_{xx}(K_1 s^2\theta + K_3 c^2\theta) + \theta_{zz}(K_1 c^2\theta + K_3 s^2\theta)\\ + (K_3 - K_1)s\theta c\theta(2\theta_{xz} - \theta_x^2 + \theta_z^2) + (K_3 - K_1)(c^2\theta - s^2\theta)\theta_x\theta_z\\ + \varepsilon_0\Delta\varepsilon(s\theta c\theta(V_z^2 - V_x^2) + (c^2\theta - s^2\theta)V_xV_z) = 0\end{aligned} \tag{9}$$

$$\begin{aligned}(\varepsilon_\perp + \Delta\varepsilon c^2\theta)V_{xx} + (\varepsilon_\perp + \Delta\varepsilon s^2\theta)V_{zz} + 2\Delta\varepsilon s\theta c\theta\\ (V_{xz} - V_x\theta_x + V_z\theta_z) + \Delta\varepsilon(c^2\theta - s^2\theta)(V_x\theta_z + V_z\theta_x) = 0)\end{aligned} \tag{10}$$

Second Case: $\phi = 90°$

Here the energy densities are given by

$$w_{\text{elast}} = \frac{1}{2}K_2\theta_x^2 + \frac{1}{2}(K_1 c^2\theta + K_3 s^2\theta)\theta_z^2 \tag{11}$$

$$w_{\text{el}} = \frac{1}{2}\varepsilon_0(\varepsilon_\perp(V_x^2 + V_z^2) + \Delta\varepsilon V_z^2 s^2\theta) \tag{12}$$

The corresponding variational equations yield

$$K_2\theta_{xx} + \theta_{zz}(K_1c^2\theta + K_3s^2\theta) + (K_3 - K_1)s\theta c\theta\theta_z^2 + \varepsilon_o\Delta\varepsilon s\theta c\theta V_z^2 = 0 \quad (13)$$

$$\varepsilon_\perp V_{xx} + (\varepsilon_\perp + \Delta\varepsilon s^2\theta)V_{zz} + 2\Delta\varepsilon s\theta c\theta V_z\theta_z = 0 \quad (14)$$

First, we discuss some pecularities of the two cases. As can be seen, the system (13), (14) is invariant with respect to a transformation $x \rightarrow -x$, while the Equations (9), (10) are changed under this transformation. Hence the director and potential distributions are symmetric with respect to the yz-plane in the case $\phi = 90°$ and asymmetric for $\phi = 0$.

Further it follows from Equation (13) that, for $\phi = 90°$, a variation of θ in the x-direction is coupled only to the elastic twist constant K_2, while in the asymmetric case, the director pattern does not depend upon K_2.

To solve the corresponding Eulerian equations numerically, a relaxation method of finite differences is used. The unit cell is divided into a grid of square meshes (lattice constant h) and the derivatives are substituted by quotients of finite differences. The functions $\theta(x, z)$ and $V(x, z)$ are approximated by arrays with elements θ_{ij} and V_{ij} given by

$$A(x, z) \rightarrow A_{ij} \quad \text{with} \quad i = [x/h], \qquad j = [y/h] \quad \text{and} \quad A = \theta, V \quad (15)$$

Here [. .] denotes the integral part of the real argument. We start the calculation by computing the matrix elements of each column using the well-known, one dimensional approach. For the two dimensional computation, a relaxation method is used which determines an iterative procedure to yield a new approximation θ_{ij}^{n+1}, V_{ij}^{n+1} from the given[11] one θ_{ij}^n, V_{ij}^n. The iteration formula are obtained from the corresponding differential equations by substituting the derivatives and solving the algebraic system for θ_{ij} and V_{ij}.

To minimize the error of discretization, the length of the meshes h should be small. This leads, however, to a bad convergence of the relaxation method. To overcome this difficulty, we have used an adapted method, accelerating the convergence rapidly. The iteration is started using a grid of a few meshes. If a given error condition is matched, the number of meshes is doubled and the solution is transferred to the new grid by interpolation. The change between iteration and interpolation is repeated until the desired discretization is achieved.

Figs. 1 and 2 show the director and voltage distribution in the unit cell in both cases for a liquid crystal layer with the following parameters: $K_1 = 11.3$ pN, $K_2 = 8$ pN, $K_3 = 12.5$ pN, $\varepsilon_\parallel = 24.8$, $\varepsilon_\perp = 6.4$, $\theta_o = 0$, $d = 10$ μm, $g = 20$ μm, $V_o = -1.0$ V. For the function $V_1(x)$, a square function with an amplitude of 1.0 V is used. One can clearly see the asymmetry and symmetry of θ and V in the cases discussed above. The figures show that the field crossing range is larger in the asymmetric case compared to the symmetric case, which is in good agreement with Reference 9. In contrast to Reference 9, the proposed numerical method allows the computation of director patterns under an arbitrary voltage distribution

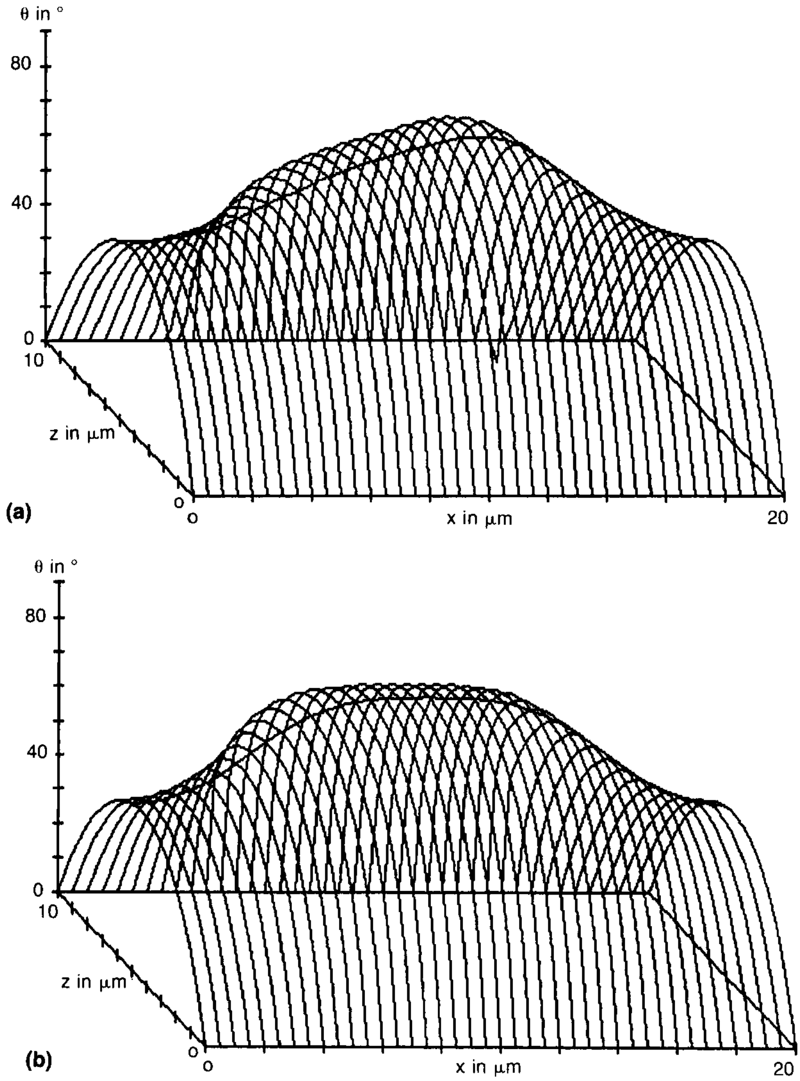

FIGURE 1 Director pattern $\theta(x, z)$ in the unit cell for the asymmetric case (*a*) and the symmetric case (*b*). Parameters given in the text.

$V_1(x)$ involving the self-consistent coupling of elastic deformation and electric field distribution.

OPTICAL PERFORMANCE OF A 2D-DEFORMED LIQUID CRYSTAL LAYER

In this section, we calculate the optical performance of the untwisted nematic layer with a given director tilt profile $\theta(x, z)$. We use the geometrical optics approximation (GOA)[12] and describe the light propagation inside the LC layer as a locally one dimensional propagation in a stratified medium. This approximation holds if

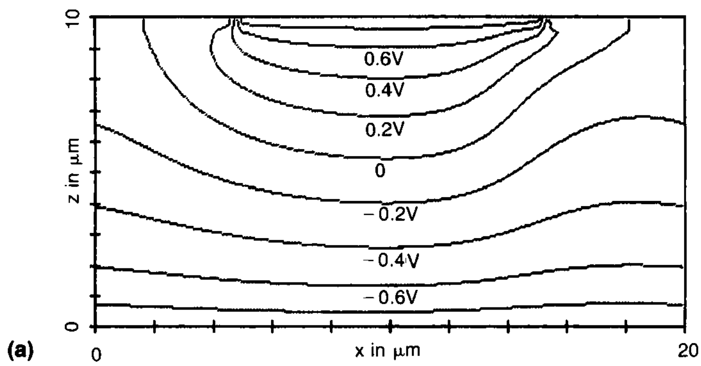

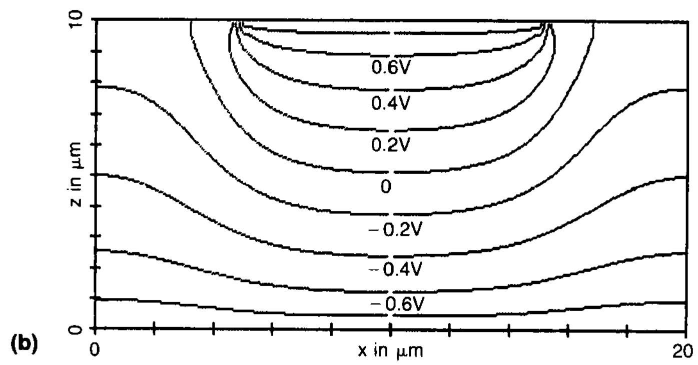

FIGURE 2 Equipotential lines of the voltage distribution $V(x, z)$ in the unit cell for the asymmetric case (*a*) and the symmetric case (*b*). Parameters given in the text.

the light is incident normally and if the director tilt profile varies slowly in the x-direction compared to the wavelength λ of the light. According to the GOA, the transmitted intensity of the light passing through the LC layer between crossed polarizers, with the director plane at 45° to the input polarizer, is given by

$$T(x) = \sin^2\left(\frac{\pi d}{\lambda}\left(\bar{n}_{e,\mathrm{eff}}(x) - n_o\right)\right) \tag{16}$$

with

$$\bar{n}_{e,\mathrm{eff}}(x) = \frac{1}{d}\int_o^d \frac{n_e n_o}{\sqrt{n_o^2\cos^2\theta(x, z) + n_e^2\sin^2\theta(x, z)}}\, dz \tag{17}$$

Here, λ denotes the wavelength of the incident light, and n_o and n_e are the refractive indices of the ordinary and extraordinary wave, respectively. $\bar{n}_{e,\mathrm{eff}}(x)$ is called the average effective extraordinary index at the position x. The described approximation was used by Nicholson[13] to calculate microscopic pictures of LC textures.

Now we consider the Fraunhofer diffraction at the LC layer that arises from the variation of the complex field amplitudes at $z = d$. We assume that the light is polarized parallel to the plane of the director—this means that only the extraordinary wave propagation must be considered and within the GOA there exists a phase grating at $z = d$. The intensity profile in the Fourier plane of a converging lens is given within the GOA by

$$I(\bar{u}) = \left| \frac{1}{Ng} \left(\frac{1 - e^{2\pi i g N \bar{u}}}{1 - e^{2\pi i g \bar{u}}} \right) \int_o^g e^{ik_o d \bar{n}_e(x) + 2\pi i x \bar{u}} \, dx \right|^2 \tag{18}$$

with the normalized diffraction angle $\bar{u} = \alpha n/\lambda$ (α: angle of diffraction, n: refractive index of the isotropic ambient). The number N denotes the number of periods illuminated by the light.

OPTICAL PERFORMANCE AND RESOLUTION CAPABILITIES OF LC SLMs

In this section, we investigate the intrinsic resolution capabilities of liquid crystal spatial light modulators (SLMs),[8] based on the theory presented above. We consider a transmissive SLM consisting essentially of a LC layer and a photoreceptor. An input optical image activates the photoreceptor, which produces a corresponding charge image that provides the electric field for the LC readout material. The read light is modulated while propagating through the LC layer. The resolution capability and field fringing of the photoreceptor were investigated recently.[8,14] However, the influence of the LC layer was neglected. It was shown that charge diffusion and finite thickness of the photoreceptor limit the resolution to about 20 lp/mm for GaAs and 70 lp/mm for amorphous silicon.[8,15]

In this paper, we investigate the resolution capability of the LC layer alone and calculate the optical response as a function of the boundary voltage distribution $V_1(x)$.

We assume that a periodic intensity modulated stripe pattern is imaged at the photoreceptor causing a periodic boundary voltage distribution $V_1(x)$ with grating constant g. (In the following we set $V_o = 0$.) The optical response of the LC layer is then investigated as a function of the grating constant g. To characterize the resolution capability of the layer, several quantities are used. Usually the modulation transfer function

$$\text{MTF} = (I_{\text{max}} - I_{\text{min}})/(I_{\text{max}} + I_{\text{min}}) \tag{19}$$

is introduced[16] where I_{min} and I_{max} are the minimum and maximum transmittances of the read light. If the SLM is used as an element of an optical processor or in pattern recognition, the diffraction efficiency of the first order of the Fraunhofer diffraction pattern is often used to characterize the optical response.[8] To describe the asymmetric optical response expected for $\phi = 0$ we introduce the averaged

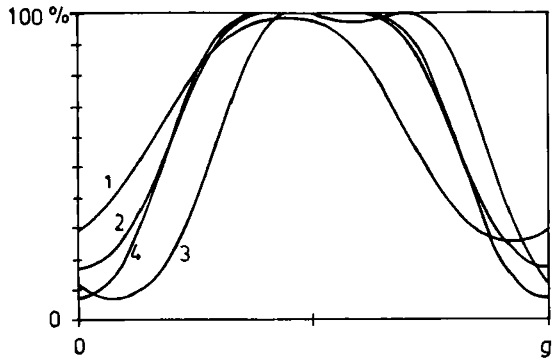

FIGURE 3 Transmittance as a function of x for light propagating normally through the LC layer, with thickness $d = 10$ μm, located between crossed polarizers. The voltage distribution is harmonic with a grating constant $g = 20$ μm. The curves 1 and 3 correspond to the asymmetric case, while curves 2 and 4 correspond to the symmetric case. Switching is between the first two extrema (curves 1 and 2) and the last two extrema (curves 3 and 4) of the one dimensional characteristics, respectively. The parameters are given in the text.

diffraction efficiency $\overline{\mathrm{DE}}$ and the asymmetric part of the diffraction efficiency ΔDE by

$$\overline{\mathrm{DE}} = (I_{+n,\mathrm{ON}} + I_{-n,\mathrm{ON}})/(2I_{\mathrm{o,OFF}}) \tag{20}$$

$$\Delta\mathrm{DE} = (I_{+n,\mathrm{ON}} - I_{-n,\mathrm{ON}})/I_{\mathrm{o,OFF}} \tag{21}$$

Here $I_{\pm n,\mathrm{ON}}$ are the intensities of the $\pm n$th order of the Fraunhofer pattern in the on-state, while $I_{\mathrm{o,OFF}}$ is the zeroth order intensity in the off-state.

In the following, we distinguish two cases of the voltage distributions $V_1(x)$. The harmonic distribution law

$$V_1(x) = \overline{V}_o + \frac{1}{2}\overline{V}_1\left(1 - \cos\left[\frac{2\pi x}{g}\right]\right) \tag{22}$$

corresponds to the first component of the Fourier expansion of an arbitrary periodic distribution. The square distribution

$$V_1(x) = \begin{cases} \overline{V}_o & \text{if } 0 \leq x \leq g/4 \quad \text{or} \quad 3g/4 \leq x \leq g \\ \overline{V}_o + \overline{V}_1 & \text{otherwise} \end{cases} \tag{23}$$

is obtained, if a binary intensity profile is perfectly transformed by the photoreceptor. We call $\overline{V}_o$ the bias voltage and $\overline{V}_1$ the amplitude of the distribution.

To investigate the resolution capability of the LC layer one has first to compute the electro-optic characteristics between crossed polarizers from the one-dimensional theory. The bias voltage $\overline{V}_o$ and the amplitude $\overline{V}_1$ are then determined by the requirement of maximum contrast and minimum response time. Usually, $\overline{V}_o$ and $\overline{V}_1$ are chosen corresponding to neighbouring extrema of the transmission *vs.*

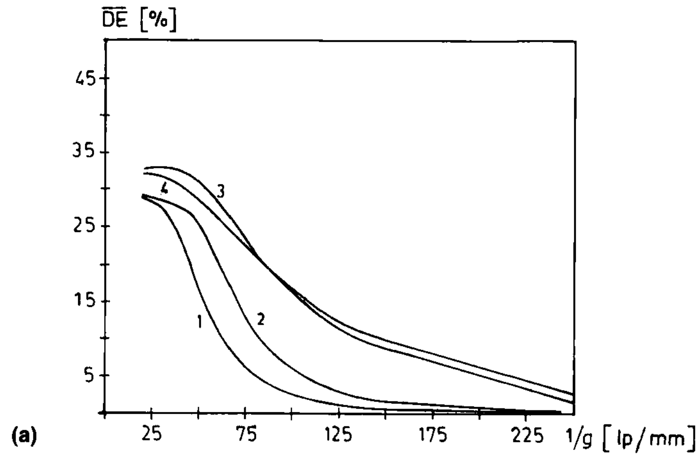

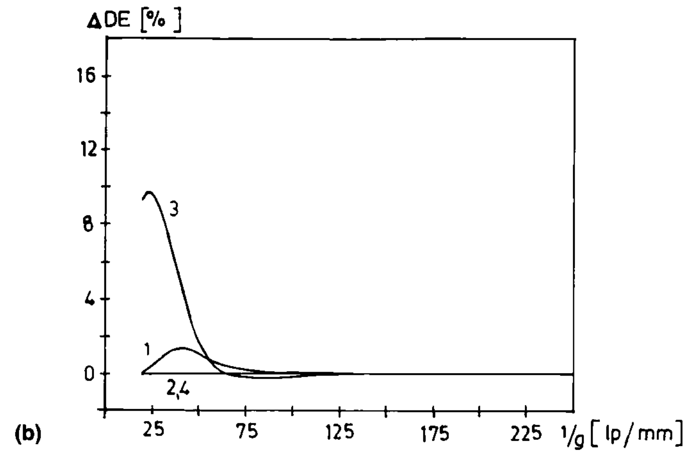

FIGURE 4 Averaged diffraction efficiency $\overline{\text{DE}}$ and the asymmetric part of the diffraction efficiency ΔDE of the first order Fraunhofer diffraction as function of the inverse grating constant. The layer has a thickness of 10 μm and the curves are named as in Fig. 3.

voltage curve. If $\overline{V}_o$ and $\overline{V}_1$ are fixed, the two-dimensional director pattern and the optical response of the layer due to a voltage distribution $V_1(x)$ are calculated as functions of the grating constant g.

To determine the influence of material and cell parameters on the resolution capability, one has first to fix $\overline{V}_o$ and $\overline{V}_1$ for each parameter set from the one-dimensional characteristics. Otherwise, a change of parameters may shift the extrema already impairing the optical performance. Now we consider a LC layer with the following material parameters: $K_1 = 11.3$ pN, $K_2 = 8$ pN, $K_3 = 12.5$ pN, $\varepsilon_\parallel = 24.8$, $\varepsilon_\perp = 6.4$, $\theta_o = 0$, $n_e = 1.610$, $n_o = 1.489$. The one-dimensional transmission *vs.* voltage characteristics of a 10 μm thick LC layer for light propagating normal to the layer having a wavelength of $\lambda = 550$ nm, exhibits four extrema, which we number beginning at the Fréedericksz transition. We compare two possible switching regions: switching between the first two extrema ($\overline{V}_o = 0.94$ V, $\overline{V}_1 = 0.27$ V), and switching between the last two extrema ($\overline{V}_o = 1.51$ V, $\overline{V}_1 = 0.76$

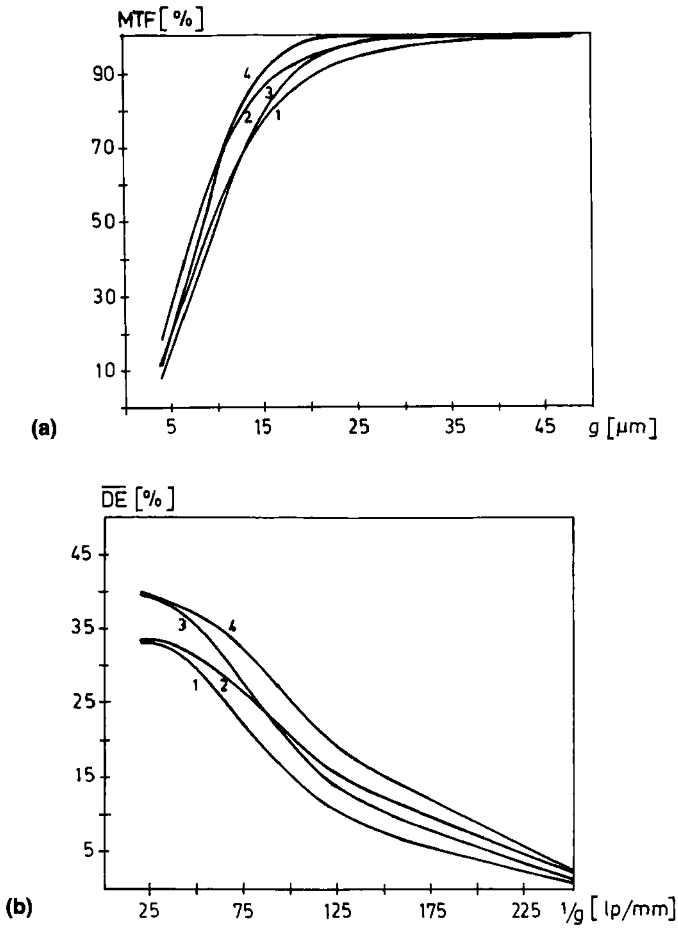

FIGURE 5 Modulation transfer function MTF as a function of the grating constant and averaged diffraction efficiency of the first order as a function of the inverse grating constant. The layer has a thickness of 5 μm and the parameters are the same as in Fig. 3. There is only one switching region with $\overline{V}_0 = 0.94$ V and $\overline{V}_1 = 0.58$ V. The voltage distribution is harmonic (curves 1 and 2) and square (curves 3 and 4), respectively. The orientation of the director is $\phi = 0$ (curves 1 and 3) and $\phi = 90°$ (curves 2 and 4), respectively.

V). Fig. 3 shows the transmitted intensity as a function of x calculated according to Equation (16), if the harmonic voltage distribution with a grating constant g = 20 μm activates the layer. Here, for each switching region, the symmetric and asymmetric cases are shown, respectively. One can see, that there is always a better imaging for $\phi = 90°$ compared to $\phi = 0$ and that for the asymmetric case, the transmission curve becomes strongly asymmetric for the high voltage switching region. This is illustrated in Fig. 4, too, which shows the averaged diffraction efficiency and the asymmetric part of the diffraction efficiency of the first order as functions of the inverse grating constant. For higher voltages, $\overline{\mathrm{DE}}$ becomes larger. However, ΔDE is increased, too, in the high voltage region for $\phi = 0$. It can be seen that ΔDE is identically zero in the symmetric case and that it vanishes in the asymmetric case if the grating constant is small or large compared to the LC

(a)

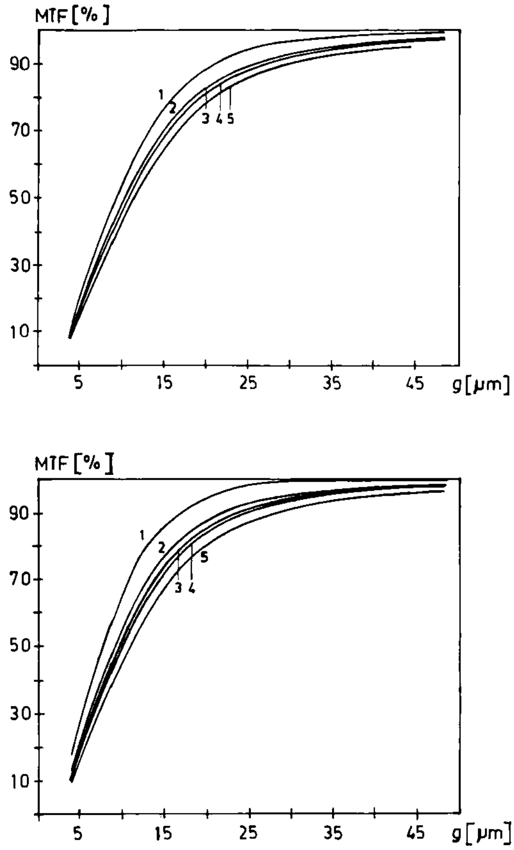

FIGURE 6 Modulation transfer function MTF as a function of the grating constant g in the asymmetric case (a) and the symmetric case (b), respectively. The layer has a thickness of 5 μm. The cell is activated by the harmonic voltage distribution and the switching region is determined for each parameter set. The parameters, except for the dielectric constants, are the same as in Fig. 3. The curves are numbered corresponding to the magnitude of the relative dielectric anisotropy: $\varepsilon_{\parallel} = 24.8$, $\varepsilon_{\perp} = 6.4$ (1); $\varepsilon_{\parallel} = 15.0$, $\varepsilon_{\perp} = 6.4$ (2); $\varepsilon_{\parallel} = 24.8$, $\varepsilon_{\perp} = 13.0$ (3); $\varepsilon_{\parallel} = 10.0$, $\varepsilon_{\perp} = 6.4$ (4); $\varepsilon_{\parallel} = 24.8$, $\varepsilon_{\perp} = 20.0$ (5).

thickness. This is clear, because for a small grating constant, the first diffraction orders vanish, while for a large grating constant, the one dimensional theory holds approximately.

The resolution capability of a LC layer becomes better if its thickness is decreased as can be seen in Fig. 5 which shows the modulation transfer function and the averaged diffraction efficiency for a layer with $d = 5$ μm. In this case, the corresponding one dimensional characteristics exhibit only two extrema; therefore only one switching region is possible. From Fig. 5, it follows that the square distribution leads to a higher diffraction efficiency compared to the harmonic distribution which is expected from ordinary Fourier optics.

Further calculations have shown that a variation of the elastic constants only weakly influences the resolution capability; the best resolution is achieved if $K_3/K_1 \approx 1$ which is in good agreement with Chigrinov.[9] On the other hand, a variation of the dielectric constants strongly affects the modulation transfer function

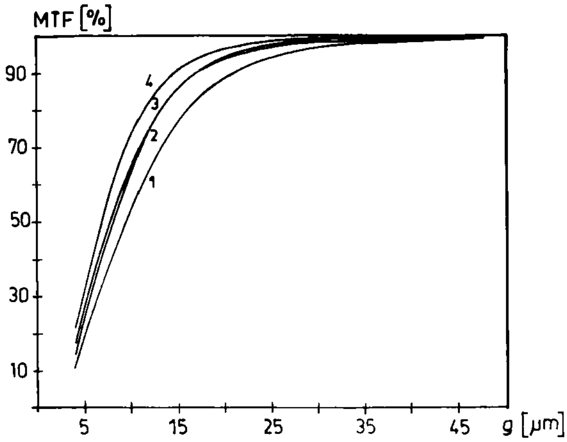

FIGURE 7 Modulation transfer function MTF as a function of the grating constant g in the asymmetric case (1, 3) and the symmetric case (2, 4), respectively. The surface pretilt is $\theta_o = 0$ (1, 2) and 10° (3, 4), respectively. The cell has a thickness of 5 μm and the parameters are chosen as in Fig. 3. For each value of θ_o the switching region is determined by the one dimensional characteristics.

especially for $\phi = 90°$ (Fig. 6). In contrast to Reference 9, we have found the best resolution capability if the relative dielectric anisotry $\Delta\varepsilon/\varepsilon_\perp$ is large. Furthermore, increasing the surface pretilt angle up to $\theta_o = 10°$ also improves the resolution (Fig. 7).

CONCLUSIONS

We have presented an original numerical computation of director configurations of a nematic liquid crystal layer in a two dimensional inhomogeneous (2D) electrical field. In the calculation, a relaxation method is used to solve the corresponding differential equations and boundary value problems. The optical performance, as exemplified by the Fraunhofer diffraction, is then calculated.

The calculations involve the self-consistent coupling between the director deformation and the electrical field distribution and were applied to LC light modulators. For the first time the anisotropy of the modulation transfer function of a nematic LC light modulator was specified and its dependence on the device parameters as well as on the LC material constants was studied. The best resolution capability is obtained if the elastic constants are equal to each other $K_3/K_1 \approx 1$ and if the relative dielectric anisotropy is large. Furthermore, the resolution is always better in the symmetric case compared to the asymmetric case. For $\phi = 90°$, the resolution is increased if K_2 is decreased.

The influence of the material parameters is greatest if the ratio between the grating constant and the layer thickness is between 2 . . . 4.

Acknowledgment

I gratefully acknowledge Prof. H. Schmiedel for many helpful discussions.

References

1. P. G. de Gennes, *The Physics of Liquid Crystals*, Clarendon, Oxford (1974).
2. D. W. Berreman, *J. Opt. Soc. Am.*, **62**, 502 (1972).
3. K. Eidner, G. Mayer, M. Schmidt and H. Schmiedel, *Mol. Cryst. Liq. Cryst.*, **172**, 191 (1989) and References therein.
4. H. Gruler, T. J. Scheffer and G. Meier, *Z. Naturforsch.*, **27a**, 966 (1972).
5. H. Deuling, *Sol. State Phys. Suppl.*, **14**, 77 (1978).
6. D. W. Berreman, *Phil. Trans. R. Soc. Lond.*, A **309**, 203 (1983).
7. H. Wöhler, G. Haas, M. Fritsch and D. A. Mlynski, *J. Opt. Soc. Am.*, A **5**, 1554 (1988).
8. D. Armitage, J. I. Thackara and W. D. Eades, *Appl. Optics*, **28**, 4763 (1989).
9. V. Chigrinov, *Mol. Cryst. Liq. Cryst.*, **179**, 71 (1990).
10. M. Schmidt and H. Schmiedel, *Mol. Cryst. Liq. Cryst.*, **167**, 89 (1989).
11. N. V. Kopchenova and I. A. Maron, *Computational Mathematics*, Mir Publishers, Moscow (1975).
12. H. L. Ong and R. B. Meyer, *J. Opt. Soc. Am.*, A **2**, 198 (1985).
13. T. M. Nicholson, *Mol. Cryst. Liq. Cryst.*, **177**, 163 (1989).
14. D. Armitage, J. I. Thackara and W. D. Eades, *Proc. SPIE*, **936**, 56 (1988).
15. D. Williams, S. G. Lathan, C. M. J. Powels, M. A. Powell, R. C. Chittick, A. P. Sparks and N. Collings, *J. Phys. D*, **21**, S156 (1988).
16. I. Abdulhalim, G. Moddel and K. M. Johnson, *Appl. Phys. Lett.*, **55**, 1603 (1989).